The American Journal of Pathology, Vol. 171, No. 4, October 2007
Copyright © American Society for Investigative Pathology
DOI: 10.2353/ajpath.2007.061164

Cell Injury, Repair, Aging and Apoptosis

Dissecting the Impact of Chemotherapy on the Human Hair Follicle

A Pragmatic in Vitro *Assay for Studying the Pathogenesis and Potential Management of Hair Follicle Dystrophy*

Enikő Bodó,* Desmond J. Tobin,† York Kamenisch,‡ Tamás Bíró,§ Mark Berneburg,‡ Wolfgang Funk,¶ and Ralf Paus*

From the Department of Dermatology, University Hospital Schleswig-Holstein, University of Lübeck, Lübeck, Germany; the Department of Dermatology,‡ Eberhard Karls University, Tübingen, Germany; Klinik Dr. Kozlowski,¶ Munich, Germany; Medical Biosciences Research,† School of Life Sciences, University of Bradford, Bradford, United Kingdom; and the Department of Physiology,§ University of Debrecen, Debrecen, Hungary*

Chemotherapy-induced alopecia represents one of the major unresolved problems of clinical oncology. The underlying molecular pathogenesis in humans is virtually unknown because of the lack of adequate research models. Therefore, we have explored whether microdissected, organ-cultured, human scalp hair follicles (HFs) in anagen VI can be exploited for dissecting and manipulating the impact of chemotherapy on human HFs. Here, we show that these organ-cultured HFs respond to a key cyclophosphamide metabolite, 4-hydroperoxycyclophosphamide (4-HC), in a manner that resembles chemotherapy-induced HF dystrophy as it occurs *in vivo*: namely, 4-HC induced melanin clumping and melanin incontinence, down-regulated keratinocyte proliferation, massively up-regulated apoptosis of hair matrix keratinocytes, prematurely induced catagen, and up-regulated p53. In addition, 4-HC induced DNA oxidation and the mitochondrial DNA common deletion. The organ culture system facilitated the identification of new molecular targets for chemotherapy-induced HF damage by microarray technology (eg, interleukin-8, fibroblast growth factor-18, and glypican 6). It was also used to explore candidate chemotherapy protectants, for which we used the cytoprotective cytokine keratinocyte growth factor as exemplary pilot agent. Thus, this novel system serves as a powerful yet pragmatic tool for dissecting and manipulating the impact of chemotherapy on the human HF. ***(Am J Pathol 2007, 171:1153–1167; DOI: 10.2353/ajpath.2007.061164)***

Chemotherapy-induced alopecia (CIA) and hair follicle (HF) dystrophy rank among the major and most frequent, unresolved problems of clinical oncology.[1–5] Although CIA has been studied since the early 1960s, using cyclophosphamide (CYP) as a lead substance,[6–9] until today no fully satisfactory preventive or therapeutic form of management is as yet available. One reason for this is that CIA presents a major therapeutic conundrum[10]: the same agents that may protect the HF from chemotherapy-induced damage may have a similar—clearly undesired—effect on tumor cells and/or are immunosuppressive. Furthermore, counteracting the chemotherapy-induced HF damage by coadministering defined agents, paradoxically, can retard full HF recovery from chemotherapy, with a subsequently much slower regrowth of normally pigmented hair shafts.[11–14]

Currently the best available model for studying and manipulating CIA *in vivo* is the mouse, and this has been instrumental for characterizing the principle features of chemotherapy-induced HF damage and its pathogenesis, for defining the distinct HF strategies to recover from it, to obtain concrete pharmacological leads for managing CIA, and for identifying key molecular players in CIA pathogenesis.[3,11,15–19] Valuable additional suggestions to pharmacological tools for managing CIA have come

Supported in part by the Deutsche Forschungsgemeinschaft (grants Pa 345/11-2 to R.P. and OTKA T049231 to T.B.).

Accepted for publication July 6, 2007.

Supplemental material for this article can be found on *http://ajp.amjpathol.org*.

Address reprint requests to Enikő Bodó, Ph.D., Department of Dermatology, University Hospital Schleswig-Holstein, University of Lübeck, D-23538 Lübeck, Ratzeburger Allee 160, Germany. E-mail: eniko.bodo@uk-sh.de.

from a neonatal rat model of CIA.[20,21] However, what is most urgently needed for therapeutic progress are clinically relevant human *in vitro* models that allow one to dissect the molecular pathogenesis of CIA and to develop new strategies for managing human CIA under physiologically relevant conditions. The current study aims to develop and characterize such an *in vitro* model, using human HF organ culture.[22] The main goal of our study was not to identify damage response pathways that are specific to chemotherapy but to develop the first human assay that recreates *in vitro* the key aspects of the histopathological characteristics published long ago by prominent dermatopathologists for the response of human scalp skin follicles to CYP treatment *in vivo*. In addition, we wished to identify a number of additional readout parameters and damage pathways whose further exploration is particularly promising for future experimental work on this topic.

Given the wealth of clinical and animal data now available on CYP-induced CIA in human and mouse,[2,6,7,9–14,17–19,23] we opted for cyclophosphamide [*cis*-(±-2-bis(2-chloroethyl)amino)tetrahydro-2-oxide-*2H*-1,3,2-oxazaphosphorine] as a reference test substance—the gold standard alkylating agent[24,25] that has long been used in clinical oncology and beyond.[2,25] *In vivo*, metabolism and activation of the drug occurs via the hepatic microsomal cytochrome P450 system. The first oxidation product of CYP is 4-hydrocyclophosphamide (4-HO-CP), which undergoes several nonenzymatic reactions.[25–27] In the absence of the hepatic cytochrome P450 system (ie, in *in vitro* studies), the most appropriate metabolite for *in vitro* study is 4-hydroperoxycyclophosphamide (4-HC), which spontaneously converts to 4-HO-CP in aqueous solution and thus generates the downstream active toxic metabolites of CYP (such as phosphoramide mustard, acrolein, and other intermediates). These preferentially target and kill cells with high proliferative activity[25,28]—including the rapidly proliferating matrix keratinocytes of the growing anagen VI HF bulb.[1–3,6] We have chosen 4-HC for our *in vitro* studies not only because it is one of the best-studied CYP metabolites but also based on several previous reports on diverse cell lines that have shown that 4-HC mimics CYP activities *in vivo* very well under *in vitro* conditions.[27,29]

The clinical histopathology of CYP-induced alopecia was characterized several decades ago[4–6,9,30,31] and has been reproduced in mice.[11,15,16] The key abnormalities of the human anagen HF in the so-called degeneration phase of CIA include atrophy of the hair matrix, tapering of the hair shaft, partial loss of inner and outer root sheath layers *in vivo*, shrinkage of the follicular dermal papilla (DP), premature apoptosis-driven[31] HF regression (catagen), and eventually, distortion of the entire HF architecture (severe HF dystrophy). The DP fibroblasts are much less affected, whereas massively and primarily affected cells are the keratinocytes of the hair matrix and the melanocytes of the HF pigmentary unit.[6,23]

The melanocytes of the HF pigmentary unit are in intimate contact with hair matrix keratinocytes and differ in several respects from epidermal melanocytes.[32–34] Only during the growth stage of the hair cycle (anagen III to VI) are melanosomes transported to the keratinocytes, whereas HF involution (catagen) is proceeded and characterized by a complete arrest of melanin production.[32–34] The melanin-producing and -transporting pigmentary unit is one of the primary targets of CIA, leading to disruption of normal melanin production and transfer (eg, abnormal transfer of pigment granules to ectopic hair bulb locations, extrafollicular melanin incontinence, disordered formation of melanosomes, and inhibition of melanosome transfer into precortical keratinocytes).[6,18,23,35,36] Such pigmentation abnormalities are not restricted to the HF, because chemotherapy can be associated with epidermal hyperpigmentation.[18] In mice, this enhanced pigmentation may result from CYP-induced proliferation and migration of the follicular melanocytes into the interfollicular epidermis.[18]

Based on insights from the C67BL/6J mouse model for CIA,[11,12] a comprehensive guide is now available that defines basic criteria for recognizing, classifying, and measuring chemotherapy-induced HF dystrophy and that summarizes the two distinct dose-dependent pathways of chemotherapy-induced HF damage (dystrophic anagen and dystrophic catagen pathways).[20] During the so-called dystrophic anagen pathway (induced mainly by a lower dose of chemotherapy), the hair shaft is shed, and the follicle undergoes an incomplete primary recovery (ie, generation of a defective hair shaft) followed by a retarded secondary recovery during which a normal hair shaft is generated. HFs that undergo the dystrophic catagen pathway (eg, in response to a higher dose of chemotherapy) immediately enter into a dystrophic catagen stage, followed by an abnormally shortened telogen phase, and thus rapid secondary recovery by premature induction of a new anagen phase. Therefore, even though it is clinically associated with the most dramatic effluvium/alopecia, the dystrophic catagen pathway leads to the fastest, complete HF recovery.[11] The principle challenge for a human *in vitro* assay for CIA research is to reproduce at least the key features of the initial stages of HF damage along these pathways.

The tumor suppressor p53 and the Fas signaling pathway (as p53 target) have been identified as pivotal players in controlling CYP-induced HF keratinocyte apoptosis in mice.[3,17,37] One challenge therefore is to study whether these controls are also important in the human system. To this end, we have used p53 immunohistology and real-time reverse transcriptase-polymerase chain reaction (RT-PCR)-verified DNA microarray technology (Human Whole Genome Oligo Microarray, 44K) to identify previously unknown target genes that may also be involved in mediating CYP-induced HF dystrophy in the human system. In view of more recent insights into the role of DNA damage in the tissue disruption caused by chemotherapy, we have also assayed for the presence of the mitochondrial DNA common deletion[38] and have screened for immunohistological evidence of DNA oxidation[39,40] in 4-HC-treated HFs.

In addition, the HF dystrophy-mitigating effect of the many agents that have been successfully used to reduce CIA or to enhance normal hair shaft regrowth in various animal models *in vivo*[11–14] now need to be validated in a

human CIA *in vitro* assay. Therefore, we opted for ideally studying the cytoprotective growth factor KGF (keratinocyte growth factor, fibroblast growth factor-7), because it strongly reduces CIA in mice,[41] is a potent survival factor for epithelial cells *in vivo*,[42,43] and inhibits massive apoptosis induced by reactive oxygen species, both in human keratinocytes *in vitro* and in organ-cultured human HFs.[44]

Materials and Methods

CYP Metabolites

4-Hydroperoxycyclophosphamide (4-HC) was obtained from Niomec (Bielefeld, Germany). Five different 4-HC concentrations (1, 3, 10, 30, and 100 μmol/L) were prepared on ice in Williams' E medium immediately before use because of the short half-life of the compound.[27] These concentrations were selected to imitate relevant serum levels of toxic CYP metabolites of patients that receive the prodrug (CYP) during normal and high-dose therapy.[45–47]

HF Organ Culture

Anagen VI HFs were microdissected and organ-cultured as described.[22,48,49] Human anagen VI HFs were isolated from excess normal human scalp skin obtained from female patients undergoing routine face-lift surgery. All experiments were performed according to Helsinki guidelines and with appropriate ethics committee approval and patient consent. Isolated HFs were maintained in supplemented, serum-free William's E medium (Biochrom, Cambridge, UK) supplemented with 2 mmol/L L-glutamine (Invitrogen, Paisley, UK), 10 ng/ml hydrocortisone (Sigma-Aldrich, Taufkirchen, Germany), 10 μg/ml insulin (Sigma-Aldrich), and 1% antibiotic/antimycotic mixture (100×; Gibco, Karlsruhe, Germany). HFs were first incubated overnight, and then the next day (day 1) medium was exchanged and vehicle/test substance was added to each well. To avoid the recognized neighboring well effect exerted by 4-HC metabolites,[27] 4-HC-treated HFs were cultured in a separate incubator from control HFs. For morphological examination, long-term cultures were performed (5 days), whereas short-term experiments (48 hours) were used for the investigation of cellular CYP effect. Hair shaft length was measured every second day on each individual HF, using a Zeiss (Jena, Germany) inverted binocular microscope with an eyepiece measuring graticule. Because HF growth *in vitro* may depend on the exact hair cycle stage *in vivo* during which the HFs were harvested,[50,51] only HFs that showed all of the accepted morphological criteria of anagen VI[7,52,53] were selected for organ culture. Because it is impossible to state which exact substage of human anagen VI these HFs represented (no reliable molecular markers available yet), we cannot exclude that the observed slight differences in the hair growth modulation by 4-HC (9 to 16% deviation) are attributable, at least in part, to the fact that the HFs were in different substages of anagen VI at the onset of culture.

To study the possible tissue-protective effect of KGF, isolated HFs were incubated overnight and pretreated with KGF (20 ng/ml; R&D Systems, Wiesbaden-Nordenstadt, Germany) for 24 hours followed by the 4-HC treatment (10 or 30 μmol/L) for 2 or 4 more days. These 4-HC concentrations were based on the recognized serum levels of CYP metabolites[45–47] in patients *in vivo* and were selected on the basis of preparatory screening experiments (not shown here), in which these concentrations best reproduced *in vivo* effects after *in vivo* CYP therapy in humans and mice.[6,9,11,13] Because of the very limited availability of human scalp HFs for these experiments, only one selected dose of KGF could be studied, which we had previously demonstrated to counteract significantly menadione-induced HF toxicity.[44]

High Resolution Light Microscopy (HRLM) and Transmission Electron Microscopy (TEM)

Human scalp HFs incubated with 4-HC for 4 days (five HFs in each treatment group, total $n = 30$ HFs) were prepared for HRLM and TEM as previously described.[54]

Histology

After cryoembedding of cultured HFs, 8-μm-thick cryostat sections were prepared for histology. HF morphology and HF cycle staging were done on hematoxylin and eosin (H&E)-stained sections (Sigma),[49] whereas for histochemical visualization of melanin, routine Masson-Fontana stain was performed.[55] As a sensitive indicator of HF dystrophy, which becomes evident as defective melanosome formation and transfer,[11,14–16] the presence of abnormally large melanin clumps (ie, Masson-Fontana$^+$ conglomerates that were larger than keratinocyte nuclei) was counted as a useful parameter for quantitatively assessing the degree of HF dystrophy (modified after Hendrix et al[23]).

Immunohistochemistry

For the simultaneous detection of apoptotic and proliferating cells in different HF compartments after 4 days of 4-HC treatment, the Ki-67/TUNEL (terminal deoxynucleotidyl transferase-mediated dUTP nick end-labeling) staining was performed as described.[49] Proliferating matrix/epidermal keratinocytes of normal human skin and frozen sections of murine spleen were used as positive control tissues for the Ki-67/TUNEL reaction. To visualize connective tissue sheath and DP fibroblasts that underwent apoptosis, a fibroblast marker (CD 90)/TUNEL double staining was used. A similar protocol was used as in case of Ki-67/TUNEL double labeling, replacing the primary Ki-67 antibody with the mouse anti-fibroblast antibody (CD90, 1:100; Dianova, Hamburg, Germany).

HF melanocyte proliferation was assessed by NKI-beteb/Ki-67 double staining. HF cryosections were presaturated with normal goat serum (10% in Tris-buffered saline) and incubated with the primary Ki-67 antibody as described above, followed by an incubation with

the secondary rhodamine-labeled goat anti-mouse antibody (1:200, 45 minutes, room temperature; Jackson ImmunoResearch Laboratories, Soham, UK). Next, the treatment with goat normal serum was repeated and slides were incubated with the primary NKI-beteb (1:50 in Tris-buffered saline plus 2% goat normal serum; Monosan, Uden, The Netherlands) overnight at +4°C, followed by the secondary, fluorescein isothiocyanate-labeled goat anti-mouse antibody (for 45 minutes at room temperature).

Because 4-HC can act as a potent inducer of oxidative DNA damage, eg, in leukemia cell lines,[56] we wished to clarify whether DNA oxidation actually occurs in 4-HC-treated (4 days) human scalp HFs. For the immunodetection of oxidized DNA,[57,58] the presence of 8-hydroxy-2′-deoxyguanosine (8-OHdG) was assessed, using the highly sensitive tyramide signal amplification method.[49] The same technique was used for the immunodetection of p53. In both cases, endogenous peroxidases were saturated with 3% H_2O_2, followed by avidin-biotin incubation (2 × 15 minutes, Avidin/biotin blocking kit; Vector Laboratories, Burlingame, CA). After 5% normal goat serum (DAKO, Glostrup, Denmark) pretreatment, HFs were incubated with the primary mouse antibody against 8-OHdG [5 μg/ml in TNB (0.1 mol/L Tris-HCl, pH 7.5, 0.15 mol/L NaCl, and 0.5% blocking reagent), overnight at +4°C; Japan Institute for the Control of Aging, Harouka, Japan] or primary mouse p53 antibody (clone DO-1, 1:1000 in TNT plus 2% normal goat serum, overnight at +4°C; Novocastra Laboratories Ltd., Newcastle, UK). On the next day sections were incubated with a biotinylated goat anti-mouse secondary antibody (1:200, 45 minutes, room temperature; Jackson ImmunoResearch Laboratories), were then incubated with streptavidin-conjugated horseradish peroxidase (1:100, 30 minutes, tyramide signal amplification kit; Perkin-Elmer, Boston, MA) and were finally incubated with tyramide (1:50, tyramide signal amplification kit). For p53 immunostaining, UVB-irradiated (50 mJ/cm^2, ~3× minimum UV-B erythema dosis, 24 hours after irradiation) organ-cultured normal human scalp skin[59] served as positive control.[60]

To confirm whether 4-HC induces oxidative DNA alterations, the presence of an additional DNA damage marker, APE1/Ref1 (abasic endonuclease/redox factor-1), which is responsible for repairing abasic sites in DNA and for regulating the redox state of other proteins that play roles in oxidative signaling,[39,40] was visualized using the peroxidase-based avidin-biotin complex method (Vectastain Elite ABC Kit; Vector Laboratories) as described.[49] Frozen sections were fixed in 4% formalin and rinsed (phosphate-buffered saline supplemented with Tween 20, PBST; Merck, Darmstadt, Germany) and endogenous peroxidase activity was saturated with 0.3% H_2O_2 in methanol for 15 minutes. Sections were incubated with normal horse serum for 30 minutes and then with the primary mouse anti-APE1/Ref1 antibody (1: 200 in PBST, 30 minutes, in humidified chamber; Kamiya Biomedicals, Seattle, WA). After the incubation with a biotinylated horse anti-mouse antibody (30 minutes), sections were treated with Vectastain ABC reagent and visualized with Nova Red substrate (Vector Laboratories). The immunoreactivity was quantitated in previously defined reference regions of the HFs, as indicated in the figure legends, using the ImageJ software (National Institutes of Health, Bethesda, MD).

Detection of Mitochondrial Common DNA Deletion

To study whether 4-HC treatment induces the mitochondrial common DNA deletion, HFs were incubated with vehicle or 30 μmol/L 4-HC for 24 hours. HFs were homogenized, and genomic DNA was isolated by the Wizard SV genomic DNA purification system (Promega, Mannheim, Germany) following the manufacturer's instructions. Detection of the common deletion was performed as described previously[38,61] and levels of the common deletion and undeleted mitochondrial DNA sequences were detected with real-time PCR. The normalized level of common deletion in vehicle-treated follicles (=1) was compared with the normalized common deletion level of 4-HC-treated follicles.[62]

Quantitative Hair Cycle Histomorphometry

HF cycle staging was performed according to previously defined morphological criteria,[7,52,63] and the percentage of HFs in anagen, early, mid, or late catagen was determined. To quantify the overall changes in HF cycling, a standardized hair cycle score[64] was calculated [score: anagen VI follicles: 100, early catagen: 200, mid-catagen: 300, and late catagen: 400, and sum of scores/group was divided by the number (n) of HFs].

Microarray and Real-Time Quantitative RT-PCR Analysis of Selected Candidate Genes

Gene expression analysis of HFs from two different individuals using Human Whole Genome Oligo Microarray (44K) was performed as a commercial service by Miltenyi Biotech GmbH (Cologne, Germany). Twenty HFs per group were treated with vehicle/4-HC (30 μmol/L) for 48 hours, total RNA was isolated according to standard protocols (TRIzol; Invitrogen). Quality of total RNA was controlled via the Agilent 2100 BioAnalyzer system (Aglient Technologies, Palo Alto, CA). Linear amplification of RNA and hybridization of whole-genome oligo microarray was performed according to the manufacturer's standard protocols. All compared test and control HFs were derived from one defined scalp skin region of the same donor, and the gene expression profiles of two donors were compared independently. Candidate genes were selected according to the following rigid selection criteria: only those genes whose transcription had changed more than fivefold (and in addition, more than twofold), in an equidirectional manner (ie, whose transcription was significantly up- or down-regulated in both individuals) and with a P value of <0.0001 were further evaluated.

The products of genes selected according to these criteria were then subjected to real-time quantitative RT-PCR (Q-PCR) analysis of separate RNA extracts derived from a third female individual, using an ABI Prism 7000

sequence detection system (Applied Biosystems, Foster City, CA) and the 5′ nuclease assay.[49] From control and 4-HC-treated HFs (20 per group), total RNA was isolated using TRIzol (Invitrogen). Then, 3 μg of total RNA were reverse-transcribed into cDNA by using 15 U of AMV reverse transcriptase (Promega, Madison, WI) and 0.025 μg/μl random primers (Promega). PCR amplification was performed by using the TaqMan primers and probes (recognizing the following human genes: assay ID Hs00170677_m1 for GPC6; Hs00181643zjh010077412. htmm1 for CTNND2; Hs00224208_m1 for SMYD3; Hs00215450_m1 for COH1; Hs00818572_m1 for FGF18; Hs00205417_m1 for B1; and Hs00174103_m1 for IL8) using the TaqMan Universal PCR Master Mix protocol (Applied Biosystems). As internal controls, transcripts of glyceraldehyde 3-phosphate dehydrogenase (GAPDH) were determined (assay ID: Hs99999905_m1 for human GAPDH).

Statistical Analysis

Data were analyzed using the Mann-Whitney *U*-test, and *P* values <0.05 were regarded as significant differences.

Results

4-HC Inhibits Hair Shaft Elongation at High Concentrations

In the current study, we wished to establish and characterize an *in vitro* human model for CYP-induced HF damage. To overcome the evident lack of a CYP-toxifying hepatic cytochrome P450 system in this *in vitro* assay, the microdissected, organ-cultured HFs were treated with 4-HC. This spontaneously converts to a cocktail of active, toxic CYP metabolites, thus mimicking the *in vivo* effects seen after CYP administration to humans.[27] HF organ cultures were treated for 4 days with a wide concentration range (0 to 100 μmol/L) of 4-HC that had been selected to reach relevant serum levels of toxic CYP metabolites as they are found in patients that receive the prodrug during normal and high-dose CYP therapy.[45–47]

As shown in Figure 1, lower concentrations (1, 3, and 10 μmol/L) did not significantly alter hair shaft elongation during the culture period. Higher concentrations (30 and 100 μmol/L), instead, caused significant ($P < 0.001$) inhibition of hair shaft elongation, whereas 100 μmol/L 4-HC arrested hair shaft growth immediately during the first treatment period.

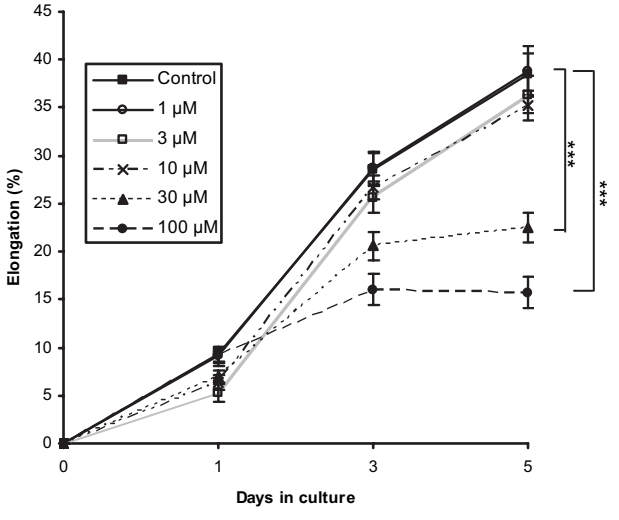

Figure 1. 4-HC inhibits hair shaft elongation at high concentrations. Isolated HFs were treated with vehicle/4-HC (1 to 100 μmol/L) for 5 days in supplemented Williams' E medium. Hair shaft length (distance between the base of the bulb and the cut end of the hair fiber) was measured every 2nd day. Hair shaft elongation (percent) of the treated groups was calculated and compared with those of the control. Elongation data are expressed as mean ± SEM, significance was calculated by Mann-Whitney *U*-test, ***$P < 0.001$. Data represents pooled results of three independent experiments.

4-HC Induces Premature Catagen-Like HF Transformation

In vivo, CYP treatment in humans and mice exerts dose-dependent damaging effects on anagen HFs and forces these to enter either into the dystrophic catagen or the dystrophic anagen pathway.[11,23] Therefore, it is important to note that 4-HC indeed induced premature catagen-like

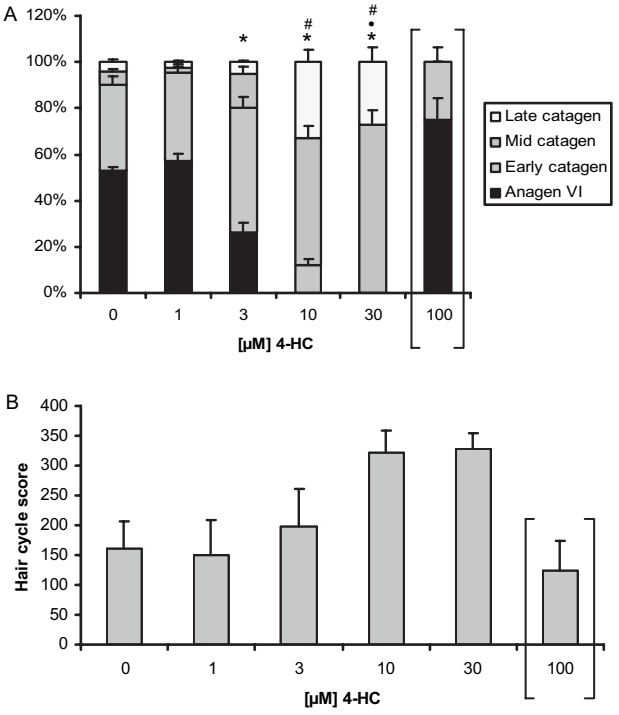

Figure 2. 4-HC induces premature catagen-like transformations. HFs were treated with vehicle/4-HC (1 to 100 μmol/L) and morphological changes were recorded on H&E-stained cryosections according to well-defined criteria. **A:** Quantitative histomorphometry shows the percentage of HFs in distinct HF stages (anagen, early catagen, mid-catagen, late catagen at day 5). **B:** Hair cycle score was calculated as follows: each HF was ascribed an arbitrary value (anagen, 100; early catagen, 200; mid-catagen, 300; and late catagen, 400). Values were added within a group and divided by the number of staged follicles. All data represent the results of three independent experiments (10 to 18 follicles/per experiment) and are expressed as mean ± SEM. Statistical analysis was performed using the Mann-Whitney *U*-test, *$P < 0.05$ in anagen, •$P < 0.05$ in early catagen, #$P < 0.05$ in mid-catagen. [ ] HFs arrest in a highly dystrophic pseudo-anagen VI stage.

development in a dose-dependent manner (Figure 2, A and B), as revealed by quantitative hair cycle histomorphometry[64]: just as we had previously shown for mice *in vivo*,[11] increasing 4-HC concentrations increased the percentage of catagen follicles (Figure 2A), along with an increase in the diameter of the DP compared with the total hair bulb diameter as a result of hair matrix shrinkage (data not shown).

In contrast, 80% of HFs treated with 100 μmol/L 4-HC were arrested in a highly dystrophic, both necrotic and apoptotic pseudo-anagen VI stage, suggesting that these maximally damaged HFs had become incapable of regular catagen-associated organ remodeling and involution because of massive, 4-HC-induced tissue death (Figures 2 and 5, see below). Interestingly, the lowest 4-HC dose tested (1 μmol/L) slightly (although nonsignificantly) increased the percentage of anagen VI HFs and reduced that of late catagen HFs compared with the vehicle control (Figure 2). This suggests that a lower level of chemotherapy-induced damage induced the dystrophic anagen—just as is seen in murine HFs *in vivo*.[11,23]

4-HC Inhibits Matrix Keratinocyte Proliferation and Stimulates Apoptosis in Selected Chemotherapy-Sensitive HF Compartments

As a result of their alkylating properties, active CYP metabolites preferentially kill cells with high proliferative potential.[23,27,28] This effect was fully reproduced in our *in vitro* assay. Quantitative Ki-67/TUNEL double immunostaining performed on HFs exposed to 4-HC for 4 days showed that CYP metabolites significantly and dose dependently decreased the absolute number of proliferating (ie, Ki-67$^+$) hair matrix keratinocytes and, in parallel, drove them into apoptosis (Figure 3, A–F, I, and K). Interestingly, the relative number of proliferating hair matrix keratinocytes (number of Ki-67$^+$ cells/number of DAPI$^+$ cells × 100; Figure 3J) showed a peak at 1 μmol/L. Intriguingly, the presence of proliferating HF pigmentary unit melanocytes could be demonstrated in the precortical matrix of 4-HC (3 μmol/L)-treated HFs by double-immunolabeling (Figure 3Ci), just as had previously been shown in CYP-treated mice *in vivo*.

Drug-induced apoptosis was not entirely restricted to the keratinocyte region, because TUNEL$^+$ cells were also identified in the HF connective tissue sheath (Figure 3K), which also harbors other cells besides specialized fibroblasts, eg, mast cells, macrophages, endothelial cells, and dermal dendrocytes. Thirty μmol/L 4-HC even induced programmed cell death in a few cells (~3) of the HF DP (as revealed by the fibroblast marker/TUNEL double staining; Figure 3, G, H, and K), which was elevated to 30% at 100 μmol/L. However, as expected from the reported clinical histopathology of CYP-treated HFs,[6] lower dose 4-HC treatment did not significantly stimulate apoptosis in HF fibroblasts (ie, the number of TUNEL$^+$/CD90$^+$ double-positive fibroblasts in the CTS and the DP of 4-HC-treated did not differ significantly from vehicle controls, data not shown). These findings suggest that, depending on the actual dose of therapeutic agent that reaches the HF, drug-induced cell death is not restricted just to the highly damage-sensitive, rapidly proliferating hair matrix, but also affects the HF mesenchyme. This may impair the crucial inductive properties of the HF fibroblasts, which are essential for anagen maintenance.[6,52,65]

4-HC Induces HF Dystrophy, as Evidenced by Disrupting Follicular Pigmentation

The most easily detectable and sensitive morphological sign of CYP-induced damage of C57BL/6J murine and human HFs is the disruption of melanin accumulation and transfer.[23,35,16,66] When HF melanin was visualized by Masson-Fontana histochemistry (Figure 4), HFs treated with 1 or 3 μmol/L 4-HC showed primarily normal pigmentation: neither ectopic melanin granules nor melanin clumping were detected (Figure 4, A–C). The first melanin clumps (reflecting melanin granule fusion and pathological extracellular melanin deposits) appeared after treatment with 10 μmol/L 4-HC, whereas 30 μmol/L essentially destroyed melanin production by the HF pigmentary unit (Figure 4, D and E). The quantification of pathological melanin production showed a significant increase in the number of melanin clumps (Figure 4G). In the group treated with 100 μmol/L 4-HC, melanin was even localized in the HF mesenchyme (ie, in the DP, although they were not seen in the CTS) (Figure 4F).

HRLM and TEM Show Severe Ultrastructural Changes in Diverse Cell Types of Human HF after 4-HC Administration

Next, the effects of 4 days of 4-HC administration on the epithelium, pigmentary system, and mesenchyme of organ-cultured normal human anagen VI HFs was further investigated by HRLM and TEM. Vehicle-treated HFs showed perfectly normal anagen VI morphology, characterized by an optimal invagination of a voluminous, onion-shaped HF DP that is fully embedded into a maximally proliferating epithelial hair bulb matrix (Figure 5a, i–v). The pigmentary units of these HFs contained multiple melanogenically active and dendritic hair bulb melanocytes and showed evidence of efficient, orthotopic transfer of melanin granules to surrounding, closely adjacent hair matrix and precortical matrix keratinocytes (Figure 5a, ii–iv). DP fibroblasts showed their normal ultrastructure[67] and were embedded in copious extracellular matrix (Figure 5av).

The addition of 1 μmol/L 4-HC was associated only with minor changes in HF morphology and ultrastructure (Figure 5b, i–v), including a reduction in matrix keratinocyte proliferation with a resultant reduction in hair bulb matrix volume. Although the pigmentary unit of these HFs retained melanogenically active HF melanocytes, these cells tended to be less dendritic and exhibited some clumping of stage IV melanosomes (Figure 5b, iii and iv). This change was associated with a reduction in the efficiency of melanin transfer to surrounding, often poorly adherent, matrix and precortical keratinocytes (Figure

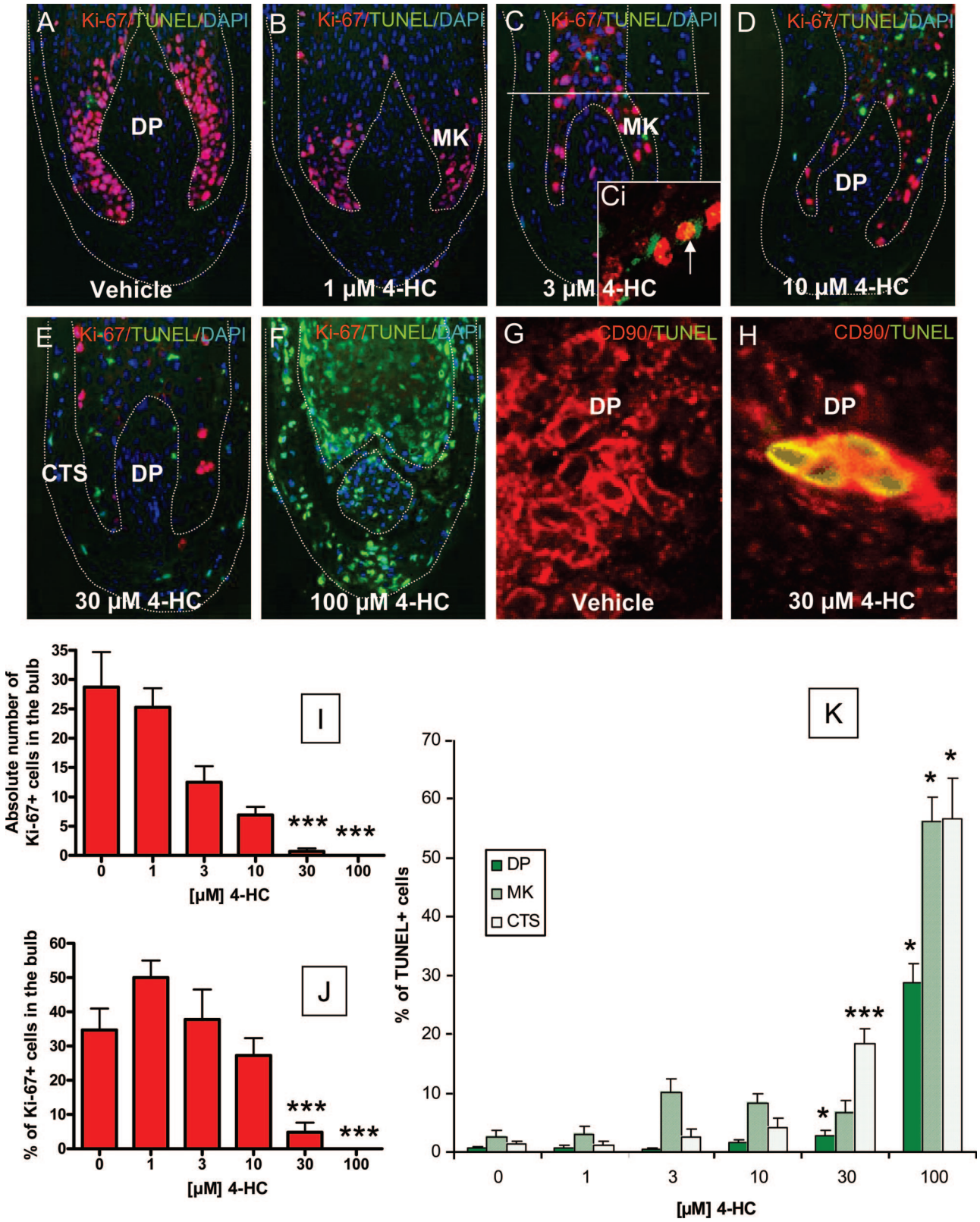

Figure 3. 4-HC inhibits matrix keratinocyte proliferation and stimulates apoptosis in several HF compartments. **A–F:** HFs were double-labeled with Ki-67 (red)/TUNEL (green) and counterstained with DAPI (blue). Ki-67-positive cells were counted in the matrix keratinocytes below the distal end of the DP (**C**) and are expressed as relative number (**I**) or percentage of all (DAPI $^{+}$) cells (**J**). **K:** TUNEL-positive cells were analyzed in two additional compartments: DP and CTS. MK, matrix keratinocytes; Ci, NKI-beteb (melanocyte marker)/Ki-67 double staining. **Arrow** denotes double-stained melanocyte. Note the proliferative HF pigmentation unit melanocytes in the precortical matrix of 4-HC (3 μmol/L)-treated HFs, as previously reported by Sharov and colleagues[18] for CYP-treated mice *in vitro*. **G** and **H:** Fibroblast marker (red)/TUNEL (green) double staining. Data are expressed as mean ± SEM. Statistical analysis was performed using the Mann-Whitney *U*-test, $^{*}P < 0.05$, $^{***}P < 0.001$. Original magnifications: ×200 (**A–F**); ×400 (**G** and **H**).

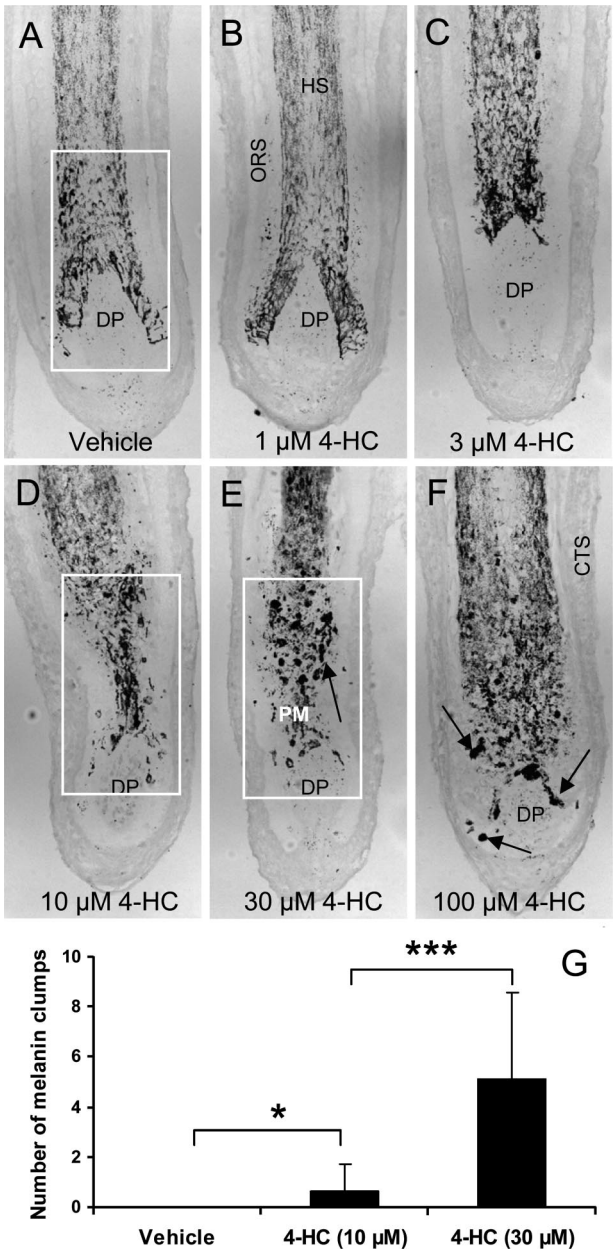

Figure 4. 4-CH induces dystrophic melanin production and transfer. **A–F:** Cultured HFs were embedded and processed for histology. Melanin granules were detected. **G:** Masson-Fontana$^+$ conglomerates that were larger than keratinocyte nuclei were counted in the defined region (indicated in white). CTS, connective tissue sheath; ORS, outer root sheath; HS, hair shaft; PM, precortical matrix. $^*P < 0.05$, $^{***}P = 0.000$. Original magnifications, ×100.

5biii). Exposure to 1 μmol/L 4-HC also induced cell stress in the DP fibroblast, as evidenced ultrastructurally by increased cytoplasmic lipid droplets and vacuolation (Figure 5bv).

As expected HF exposure of HFs to 3 μmol/L and 10 μmol/L 4-HC caused much more dramatic morphological/ultrastructural changes (Figure 5, c and d). These included involution and retraction of the HF epithelium in a catagen-like manner (Figure 5, ci and di), a marked disruption of the HF pigmentary unit, and a significant vacuolation of hair bulb keratinocytes and HF melanocytes at the matrix-DP junction (Figure 5cii). Cell death, with the morphological features of apoptosis, was commonly seen in the hair bulb matrix of these HFs and was more commonly found in the HF keratinocyte, than in the melanocyte (Figure 5c, ii–iv; and Figure 5d, ii and iii). Active melanogenesis was still observed in 4-HC-treated HF melanocytes (Figure 5, civ and div), although transfer of melanin to surrounding keratinocytes was impaired. Significant cellular stress was apparent in the DP fibroblasts under these conditions, as evidenced most impressively by the presence of giant lysosomal structures containing lipidic material in addition to cellular debris (Figure 5, cv and dv).

Exposure of anagen VI HFs to 4-HC at 30 and 100 μmol/L also induced HRLM and TEM features of necrosis (Figure 5e, i–v; and f, i–v). At 30 μmol/L, HFs appeared to have undergone a (apoptosis) catagen-like change for some time before this necrosis ensued, as indicated by signs of epithelial cell retraction and substantial shrinkage of the hair matrix volume (Figure 5ei). By contrast, HFs exposed to 100 μmol/L 4-HC retained a pseudo-anagen VI morphology indicating that necrosis occurred very soon after the commencement of 4-HC exposure, rendering such catagen-like organ transformations impossible (Figure 5f).

p53 Seems to Be Involved in 4-HC-Induced Human HF Dystrophy

As a first step toward dissecting the possible mechanisms of the CYP-induced HF damage in the human system, p53 immunoreactivity was studied because p53 is an essential mediator of CIA and HF dystrophy in C57BL/6J mice.[17] Using a monoclonal p53 antibody that recognizes both wild-type and mutant forms of human p53,[68] no p53-positive cells were found in the vehicle-treated control HFs (neither in anagen, nor in catagen HFs) (Figure 6A). Instead, as shown in Figure 6, B–G, 4-HC significantly and dose dependently up-regulated the number of immunohistologically detectable p53$^+$ cells in the epithelial matrix keratinocytes, whereas a few p53$^+$ could also be seen in the CTS, outer root sheath, and sometimes even in the DP, depending on the 4-HC dose used.

4-HC Induces the Mitochondrial Common DNA Deletion

Given that CYP metabolites act as alkylating agents mainly because of cross-linking of strands of DNA,[24,25] we further investigated 4-HC-induced DNA changes. Acquired mitochondrial DNA mutations are typically mediated through reactive oxygen species,[69] which persist as long-term *in vivo* markers in human skin.[70] When HFs were isolated from three different human individuals and exposed to 30 μmol/L 4-HC in organ culture, compared with the vehicle group, a massive induction of mitochondrial common DNA deletion was observed in two of the three experimental groups, fluctuating between a 100-fold increase (experiment 3) and an ~3000-fold increase

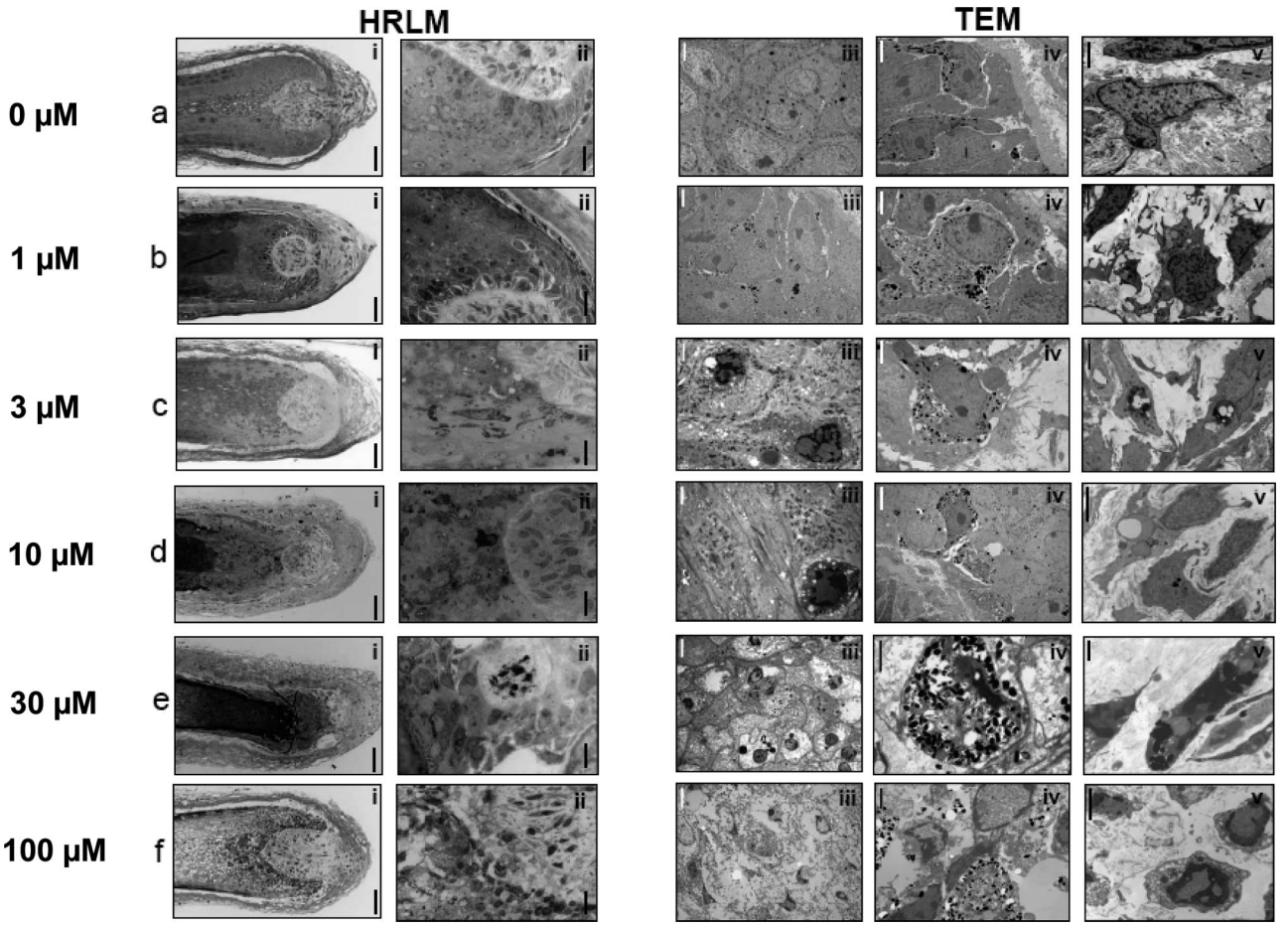

Figure 5. HRLM (**i** and **ii**) and TEM (**iii–v**) show severe ultrastructural changes in diverse cell types of human HF after 4-HC administration. **a:** No exposure to 4-HC. HFs exhibited normal anagen VI morphology and ultrastructure including dispersion of DP cells in copious extracellular matrix (**i** and **v**) and an intact HF pigmentary unit (**ii** and **iv**). Keratinocyte differentiation appeared normal (**iv**), although some thickening of the basal lamina separating the DP and the matrix was apparent (**iv**). **b:** Exposure to 1 μmol/L 4-HC. HFs exhibited anagen morphology and ultrastructure with some loss of matrix volume (**i**). DP cells were dispersed in copious extracellular matrix (**i** and **v**) and the HF pigmentary unit appeared intact (**ii** and **iv**). Keratinocyte differentiation appeared normal (**iv**) and proliferation among matrix keratinocytes was evident (**ii**). **c:** Exposure to 3 μmol/L 4-HC. HFs exhibited early catagen-like morphology and ultrastructure including some loss of matrix and DP volume (**i** and **v**). DP cells contained large vacuoles and phagolysosomal inclusions (**v**). The HF pigmentary unit displayed some perturbation including pigment accumulation, which suggested a reduction in melanin transfer efficiency (**ii**). Scattered degenerating keratinocytes were found in the HF precortex. **d:** Exposure to 10 μmol/L 4-HC. HFs exhibited advanced catagen-like morphology and ultrastructure including a substantial loss of matrix and follicular papilla volume (**i** and **v**). DP cells were distributed in a clumped manner and contained large vacuoles and phagolysosomal inclusions, some containing melanin (**v**). The HF pigmentary unit contained some intact and functioning melanocytes, whereas other melanocytes exhibited degenerative change (**ii**). Scattered degenerating keratinocytes were detected in the HF precortex. **e:** Exposure to 30 μmol/L 4-HC. HFs exhibited a dystrophic catagen-like morphology and ultrastructure including a substantial loss of hair bulb epithelial volume and DP volume (**i** and **v**). DP cell number seemed to be reduced, and some cells appeared necrotic and were observed to contain numerous large inclusions (**v**), some of which contained melanin and lipid-like inclusions. The HF pigmentary unit was severely disputed with little evidence of functioning melanocytes remaining. Degenerating melanocytes were also detected high in the precortex, after detachment from the hair bulb (**iv**). Keratinocytes of the precortex and cortex displayed evidence of widespread necrosis (**iii**). **f:** Exposure to 100 μmol/L 4-HC. HFs exhibited a complete cytotoxic stasis characterized by a pseudo-anagen morphology derived from completed necrotic change in all cellular compartments.

(experiment 2) (Figure 6N). These large interindividual variations with regard to the induction of the DNA common deletion may mirror the interindividual differences in the alopecia-related chemotherapy sensitivity that is typically observed in clinical oncology.[3]

4-HC Treatment Causes HF DNA Oxidation

Next, we searched for evidence of 4-HC-induced DNA damage by oxidation and investigated the expression of 8-hydroxy-2′-deoxyguanosine (8-OHdG), the oxidant of deoxyguanosine, which represents the most commonly used indicator of DNA oxidative damage.[57,58] Indeed, as shown in Figure 6, H–K, the intensity of 8-OHdG immunoreactivity was increased after 4-HC application in several HF compartments (matrix keratinocytes, connective tissue sheath, and DP). As an additional marker and independent evidence for oxidative DNA stress, immunostaining for Ref1/APE1 was performed on 4-HC-treated HFs, because this enzyme is involved in base excision repair after DNA damage associated with oxidative stress.[39,40] As revealed by ABC immunohistochemistry (Figure 6, L and M), 4-HC also displayed prominently up-regulated Ref1/APE1 immunoreactivity. The up-regulation of both 8-OHdG and Ref1/APE1 immunoreactivity by 4-HC was dose-dependent (not shown). Taken together, this sug-

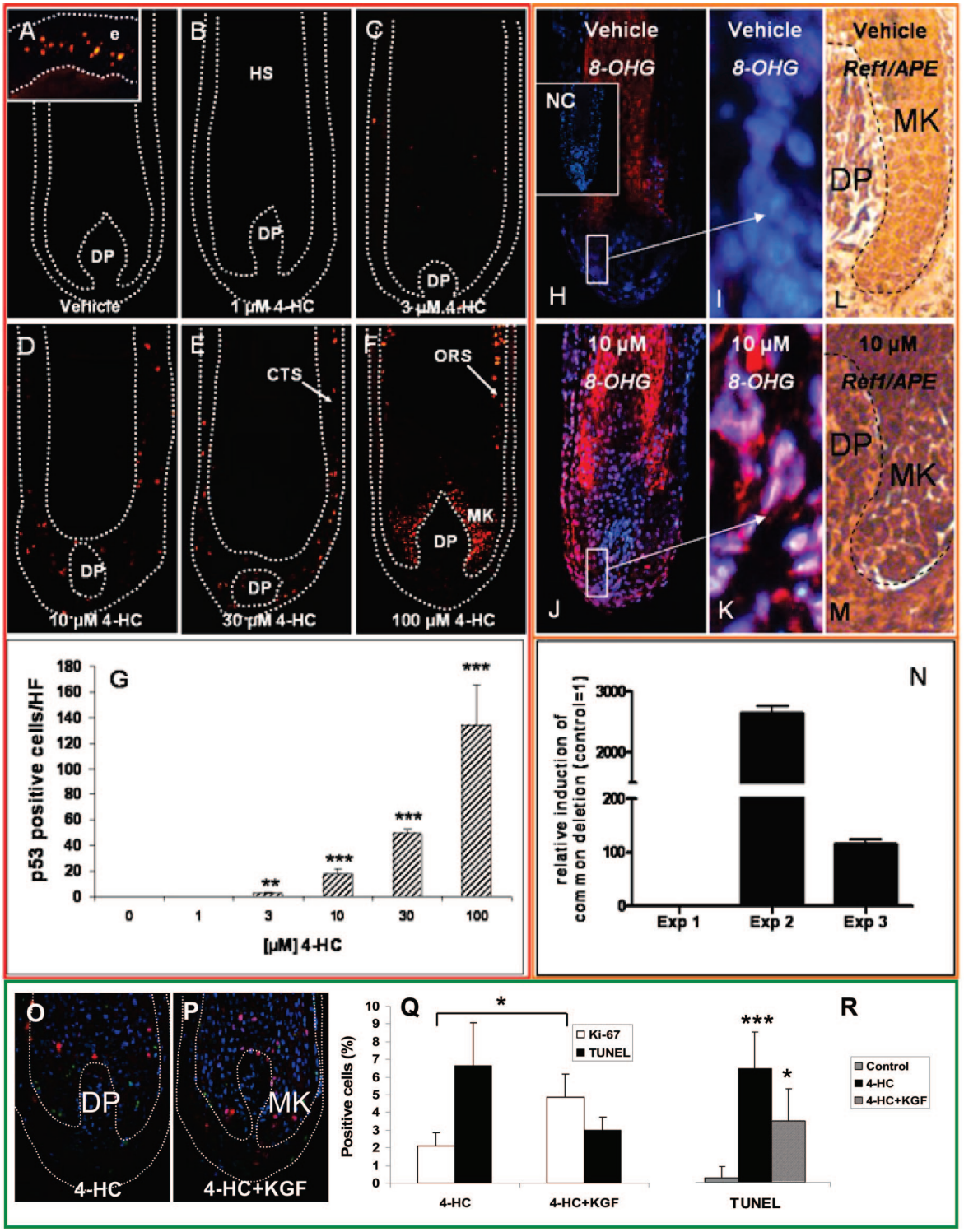

Figure 6. 4-HC increases the number of the p53-expressing cells, common DNA deletion, and DNA oxidation in a dose-dependent manner in HF organ culture. **A–G:** KGF slightly, but significantly, diminishes 4-HC-induced inhibition of hair matrix keratinocyte proliferation and inhibits 4-HC-induced HF apoptosis: HFs were treated with 4-HC (1 to 100 μmol/L), and p53 protein was detected on HF cryosections by tyramide signal amplification method. p53-positive nuclei/HFs were counted. Data are expressed as mean ± SEM, statistical analysis was performed using the Mann-Whitney *U*-test. $^{**}P < 0.01$, $^{***}P < 0.001$. e, epidermis; CTS, connective tissue sheath; ORS, outer root sheath; HS, hair shaft. **H–N:** Vehicle/4-HC-treated HFs were stained for 8-OHdG and Ref1/APE1 (specific indicators of oxidative DNA damage). NC, negative control; MK, matrix keratinocytes. **N:** HFs were incubated with vehicle/30 μmol/L 4-HC, and homogenized and genomic DNA was isolated for detection of the common deletion by real-time PCR. Relative induction of mitochondrial DNA deletion were compared with the vehicle (=1). **O** and **P:** Double labeling of proliferating (red) and apoptotic (green) cells by Ki-67/TUNEL immunohistochemistry of vehicle (**O**) and KGF (**P**) pretreated HFs exposed to 4-HC (30 μmol/L). The percentage of Ki-67- and TUNEL-positive cells is shown (**Q** and **R**) as mean ± SEM. $^{*}P < 0.05$. MK, matrix keratinocytes. **R:** Human scalp HFs were pretreated overnight with 20 ng/ml KGF before administration of 10 μmol/L 4-HC (under continued stimulation with KGF), and they were cultured for 48 more hours. The percentage of TUNEL^{+} cells was counted (mean ± SEM, $^{*}P < 0.05$, $^{***}P < 0.001$). Original magnifications: ×100 (**A–H**, **J**, and **N–R**); ×400 (**I** and **K**); and ×200 (**L** and **M**).

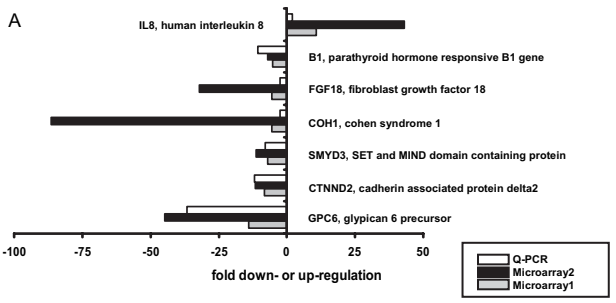

Figure 7. 4-HC alters the gene expression program of human HF. Gene expression analysis of HFs from two different individuals (Microarray1 and Microarray2) was performed using Human Whole Genome Oligo Microarray (44K). HFs (20 per group) were treated with vehicle/4-HC (30 μmol/L) for 48 hours. Candidate genes were selected according to the following criteria: equidirectional expression changes in both individuals, P value <0.0001, more than fivefold change. For a confirmation Q-PCR analysis (Q-PCR) of the above-selected genes was performed. Expression changes are displayed as fold down- or up-regulations.

gests that toxic CYP metabolites exert their HF dystrophy-inducing effects at least in part via the promotion of intrafollicular DNA oxidation.

4-HC Alters the Gene Expression Program of Human HF

To screen for possible target genes associated with CYP-induced human HF damage, we subjected two independent sets of organ-cultured human scalp HFs (derived from two different healthy female face lift patients) to DNA microarray. This was performed as a commercial service (Human Whole Genome Oligo Microarray; Miltenyi Biotech), and rigid selection criteria were used to single out differentially expressed genes. When only equidirectional expression changes in HF RNA extracts from both individuals with a P value of <0.0001 and fold changes of more than twofold were accepted as indications for differential gene expression, 101 up-regulated and 320 down-regulated genes were identified, most of which are involved in the regulation of apoptosis, cell cycle, cell structure, and/or cellular metabolism (see Supplemental Table 1, available online at *http://ajp.amjpathol.org*). Next, only genes with the highest (ie, more than fivefold) expression changes were selected, and their differential transcription was independently confirmed by real-time quantitative PCR on RNA extracts derived from HF of a third donor. This showed that 4-HC treatment for 48 hours in serum-free organ culture strongly down-regulated the following genes (Q-PCR controlled): parathyroid hormone responsive B1 (B1), fibroblast growth factor-18 (FGF18), Cohen syndrome 1 (COH1), SET and MIND domain-containing protein (SMYD3), cadherin-associated protein delta2 (CTNND2), and glypican 6 precursor (GPC6), and human interleukin 8 (IL-8) was up-regulated by 4-HC (Figure 7).

KGF Slightly, but Significantly, Inhibits 4-HC-Induced HF Apoptosis and Dystrophy and Diminishes the Inhibition of Hair Matrix Keratinocyte Proliferation

Previously, we had shown that KGF inhibits massive intrafollicular keratinocyte apoptosis in organ-cultured human HFs treated with the free radical donor, menadione.[44] Therefore, we tested the effect of KGF on 4-HC-induced HF apoptosis. When organ-cultured human scalp HFs were pretreated overnight with 20 ng/ml KGF before administration of 30 μmol/L 4-HC (under continued daily stimulation with KGF), 4 days later, the massively increased number of TUNEL$^+$ cells in the epithelial hair matrix of HFs treated only with 4-HC (6.6 ± 2.4% versus 0.5 ± 0.5% in vehicle-treated controls) was reduced by 55.34% in KGF-treated follicles (3 ± 0.75%) (Figure 6, O and P). Even though the large substantial variations in the number of TUNEL$^+$ cells in all test groups (as indicated by the large SEMs; n of HFs per group = 14 to 18) prevented the level of statistical difference being reached ($P > 0.05$). This suggests that KGF has the potential to counteract chemotherapy-induced apoptosis in the HF matrix.

An additional short-term experiment further supports the anti-apoptotic, protective activity of KGF in 4-HC-mediated HF damage (Figure 6R). Human scalp HFs were pretreated overnight with 20 ng/ml KGF. Ten μmol/L 4-HC was added under continued stimulation with KGF for an additional 48 hours. 4-HC was able to induce massive ($P < 0.001$) apoptosis already during this shorter culture period. Importantly, the KGF pre- and coadministration led to the significantly decreased number of apoptotic hair matrix cells (Figure 6R) ($P < 0.001$).

Finally, we examined the possible protective KGF effects on HF keratinocyte proliferation *in vitro*. HFs were preincubated with vehicle or 20 ng/ml KGF overnight before administering 4-HC (30 μmol/L) for 4 days. As shown by quantitative Ki-67 immunohistomorphometry, KGF slightly, but significantly ($P < 0.05$), increased the number of Ki67$^+$, proliferating hair matrix keratinocytes compared with HF that had only been treated with 4-HC (Figure 6Q).

Discussion

Here, we show that the serum-free organ culture of microdissected, normal human scalp HFs in anagen VI is perfectly suited to reproduce and dissect the impact of chemotherapy on human HFs *in vitro*. Note that the current study was not designed to dissect which of the observed damage responses of organ-cultured human scalp HFs are specific to the agent tested and which ones reflect general follicular response pathways to chemical damage. We could reproduce the key parameters of CIA-induced hair damage that has been observed using pathological biopsies[6,9,30,31,71] as summarized in Table 1, which highlights and compares published CYP-induced effects on HFs in humans *in vivo*, in mice *in vivo* and in our *in vitro* model. Using a combination

Table 1. Comparison of CYP-Induced Hair Follicle Damage in Human System *in Situ*, in Human Skin/Severe Combined Immunodeficient Model *in Vivo*, and in HF Organ Culture *in Vitro*

Parameter*	CYP-treated patients	Mouse CIA model	Human skin/severe combined immunodeficient model	HF organ culture model
Inhibition of hair shaft elongation	Decreased rate of hair shaft production[4,6,30]	Not directly investigated. Catagen induction may suggest inhibition of hair shaft elongation[11]	NA	Yes
Increased apoptosis of matrix keratinocytes	Yes[31]	Yes[17,19,91]	Yes[91]	Yes
Decreased proliferation of matrix keratinocytes	Yes, decreased mitotic activity[6,31]	NA	NA	Yes
Catagen induction	Yes[4–6,9,71]	Yes[11]	Yes[91]	Yes
Disrupted melanogenesis and melanin transfer	Disrupted: ectopic melanin granules, clumping[6,9]	Disrupted: ectopic melanin granules, clumping. Irregular banding pattern of the hair shaft[11,18,35]	NA	Yes
Involvement of up-regulated p53	NA	Up-regulated p53 protein expression, p53 knockout mice do not show CIA[17,91]	Up-regulated p53 protein expression[91]	Yes

NA, not assessed.
*Recognized key parameters relevant to the assessment of chemotherapy-induced hair follicle damage, in particular after cyclophosphamide treatment.[6,11,19,23]

of morphological and molecular techniques, we demonstrate that these HFs respond to a key CYP metabolite (4-HC) in a manner that imitates chemotherapy-induced HF dystrophy and alopecia as it occurs *in vivo*: 4-HC induces melanin clumping and incontinence, down-regulates proliferation and massively up-regulates apoptosis of (predominantly) hair matrix keratinocytes, prematurely induces catagen, and up-regulates p53. This confirms in the human system previous key features dissected for CIA in the best currently available mouse model.[11,13,17–19] (Naturally, caution is advised in directly comparing our *in vitro* results with the *in vivo* situation, because one cannot predict whether the 4-HC concentration tested in the current assay would indeed induce alopecia if administered to patients.)

In addition, we show here that chemotherapy can induce both follicular DNA oxidation and the mitochondrial DNA common deletion in human scalp HFs, and provide useful new pointers to potential target genes of chemotherapy-induced human HF damage. Moreover, this assay enables one to explore the modulatory properties of prototypic cytoprotective candidate substances (here KGF) on intact human scalp HFs.

Exactly as previously described for CYP therapy in humans[6,31] and mice[11,23] *in vivo*, 4-HC predominantly targeted matrix keratinocytes with their exceptionally high proliferative potential, where proliferation was inhibited and apoptosis massively up-regulated. This suggests that 4-HC spontaneously converts to active toxic metabolites (eg, phosphoramide mustard, acrolein, and probably others[25–27]) in the culture medium and/or HF tissue. Because phosphoramide mustard is the main alkylating agent among these metabolites,[72] it likely causes DNA cross-linking in this epithelial HF cell population, which exhibits one of the highest rates of cell proliferation of any tissue in normal mammalian biology.[52,73] However, because many studies have demonstrated that acrolein alone is also potently able to induce both necrosis and apoptosis in several cell types *in vitro*,[28,74,75] acrolein probably contributes to the observed HF-damaging effects of 4-HC. Dose-dependent apoptosis and necrosis were also detectable by immunohistology and electron microscopy in HF compartments beyond the hair matrix (including the HF mesenchyme). Thus, these toxic CYP metabolites are most probably capable of also disrupting the intimate, bidirectional epithelial-mesenchymal communication that is an essential prerequisite for anagen maintenance and normal HF cycling.[52,65,73] The reported effects of 4-HC are likely not restricted/specific for 4-HC/CYP, because most chemotherapeutic agents of the family of alkylating agents (eg, carboplatin, ifosfamide, thiotepa, busulfan[8]) all cause very similar toxicological and cell biological effects (dystrophic catagen induction, disrupted melanogenesis).[76,77] However, the specificity of the HF effects described here for 4-HC needs to be further investigated.

Patients receiving CYP therapy develop miniaturized, premature catagen HFs associated with hair matrix shrinkage and pseudo-expansion of the DP, whereas hair shaft elongation during this initial period remains almost unaltered.[3,6,7] Again, our results perfectly reproduce these well-appreciated clinical phenomena: 4-HC-treated human HFs prematurely regress and are transformed to catagen HFs, associated with a pseudo-increase in DP volume, whereas hair shaft growth is inhibited only by higher 4-HC concentrations. We cannot exclude that 4-HC, in our *in vitro* system, exerts a lower HF-damaging activity than CYP *in vivo*. Clinically, however, chemotherapy-induced hair loss typically begins 1 to 3 weeks after treatment initiation[3] and HFs develop a protracted, relatively slowly increasing dystrophic catagen transformation resulting in alopecia.[4–6,9] Because 4-HC treatment very rapidly induces catagen transformation (which necessarily is an apoptosis-driven tissue involution event[65]) (first signs already after 2 to 3 days), this strongly argues against the concept

that 4-HC *in vitro* is significantly less active than the precursor from which it is metabolized *in vivo* (CYP).

As shown, most HFs treated with 100 μmol/L 4-HC were arrested in a highly dystrophic and both necrotic and apoptotic pseudo-anagen VI stage. Because of the very high 4-HC concentration in this group, 4-HC-sensitive HF cells essentially die immediately before they have a chance to undergo the complex tissue remodeling events that are an essential prerequisite for undergoing the characteristic morphological alterations of the anagen-catagen transformation,[10] which requires perfectly viable cells/tissue. Although the exceptionally high number of TUNEL-positive cells suggests DNA fragmentation because of apoptosis, the TUNEL assay cannot exclude with certainty concomitant necrosis (only ultrastructural analysis is reliable in this respect). In fact, our TEM analyses have revealed clear-cut ultrastructural signs of necrosis, documenting that both apoptosis and necrosis are induced by this very high 4-HC concentration.

A hallmark of HF dystrophy after CYP therapy is the disrupted melanin production and transfer associated with melanin clumping, ectopic melanin location, and irregular melanin banding pattern of hair shafts.[6,9,11,23,35] As shown by Masson-Fontana histology, HRLM and TEM, the current human HF assay fully reproduces the disruption of HF pigmentation seen *in vivo* (including the previously reported proliferation of HF melanocytes after CYP treatment).[18]

This new model for studying human HF dystrophy also suggests that follicular DNA oxidation and mitochondrial DNA common deletion are relevant in the molecular pathogenesis of chemotherapy-induced human HF dystrophy. Several mechanisms may be involved in the induction of these DNA effects. 4-HC causes oxidative DNA damage (including 8-OHdG up-regulation) through H_2O_2 generation after 4-HC treatment,[56] inhibits mitochondrial oxygen consumption, and impairs cellular respiration.[78] In addition, the CYP metabolite acrolein (which also generated from 4-HC *in vitro*[27]) induces oxidative stress by depleting glutathione or by nuclear alkylation reactions.[28,79] Furthermore, acrolein decreases mitochondrial enzyme activities (mitochondrial complexes I, II, and III; superoxide dismutase; and glutathione peroxidase).[80] Our results furthermore encourage one to explore the chemotherapy-protective effects of antioxidants (ie, vitamin E, β-carotene, and melatonin)[69,81,82] that have been shown to protect from reactive oxygen species-induced mitochondrial DNA damage to protect selectively human scalp HFs (eg, after topical application in HF-targeting liposomes[83–86] from chemotherapy-induced oxidative and structural mitochondrial and nuclear DNA damage).

The relative apoptosis-protection awarded by KGF further shows that our assay can also be used as a tool for identifying and testing the effects of other candidate chemotherapy protectants directly in the relevant human target organ *in vitro*. Thus, this novel assay serves a powerful, yet pragmatic tool for dissecting and manipulating the impact of chemotherapy on the human HF under well-controlled, serum-free, physiologically relevant conditions that mimic key aspects of the clinical situation as closely as this is currently possible *in vitro*.

Using standard DNA microarray technology, we could also identify new molecular targets for chemotherapy-induced HF damage, whose relative importance in the pathogenesis of HF dystrophy now needs to be individually dissected in systematic follow-up studies. The main therapeutic challenge here will be to clarify whether any of these newly discovered candidate targets of 4-HC-induced HF cytotoxicity can be exploited in the future pharmacological management of CIA. Some of these genes have not been considered previously in the context of HF biology (eg, *SMYD3*, *IL-8*, *GPC6*), and open new perspectives in the molecular pathology of chemotherapy-induced HF dystrophy, whereas others are already appreciated regulators of HF cycling (eg, *FGF18*)[87,88] or have known mutations associated with distinct hair phenotype abnormalities (*COH1*).[89]

Ideally, the current *in vitro* assay should be complemented by a murine *in vivo* assay[90] that is based on the original mouse model for CYP-induced alopecia[11] yet uses human scalp skin transplanted onto immunocompromised mice. In this manner, long-term effects of chemotherapy on human HFs, in particular on their cycling, hair regrowth and repigmentation characteristics could be studied.[91] However, such complex *in vivo* assays are considerably more labor-, cost-, and time-intensive than the simple, pragmatic human *in vitro* assay reported here, and require both animal experimentation and special surgical expertise. Thus, they are much less widely accessible. An additional caveat arises from the (typically underestimated) concern that such mixed-species assays superimpose on the transplanted—exquisitely hormone-sensitive[92]—human HF many potent, but highly artificial, regulatory controls provided by host endocrine signals. This surely complicates data interpretation. For routine and large-scale CIA research purposes, the human *in vitro* assay system presented here, therefore, offers a highly pragmatic, clinically relevant, instructive, widely available, and cost-friendly experimental tool.

Acknowledgments

We thank Sabine Werner (Eidgenössische Technische Hochschule, Zurich, Switzerland) for expert advice and constructive criticism, Astrid Becker and Levente Bodó for excellent technical help, and Michael Colvin and Jim Kehrer for helpful advice.

References

1. Hesketh PJ, Batchelor D, Golant M, Lyman GH, Rhodes N, Yardley D: Chemotherapy-induced alopecia: psychosocial impact and therapeutic approaches. Support Care Cancer 2004, 12:543–549
2. Fraiser LH, Kanekal S, Kehrer JP: Cyclophosphamide toxicity. Characterising and avoiding the problem. Drugs 1991, 42:781–795
3. Wang J, Lu Z, Au JL: Protection against chemotherapy-induced alopecia. Pharm Res 2006, 23:2505–2514
4. Merk HF: Drugs affecting hair growth. Biology of the skin and hair growth. Edited by AG Lyne, BF Short. Sydney, Augus and Robertson, 1965, pp 601–609
5. Crounse GR, van Scott EJ: Changes in scalp hair roots as a measure of toxicity from cancer chemotherapeutic drugs. J Invest Dermatol 1960, 35:83–90
6. Braun-Falco O: Klinik und pathomechanismus der endoxan-alopecie

als beitrag zum wesen cytostatischer alopecien. German. Arch Klin Exp Dermatol 1961, 212:194–216
7. Whiting D: Histopathology of alopecia areata, a new look. Arch Dermatol 2003, 139:1555–1559
8. Calabresi M, Anerein PC, Drucker BJ, Michaelson MD, Mitsiades CS, Gros PE, Ryan DP, Ramachandra S, Richardson PG, Supko JG, Wilson WH: Chemotherapy of neoplastic diseases. Goodman and Gilman's The Pharmacological Basis of Therapeutics. Edited by E Brunton, JS Lazo, KL Parker. New York, McGraw-Hill Publishing Co., 2005, pp 1315–1403
9. Kostanecki W, Kwiatkowska E, Zborzil J: Hair melanogenesis in endoxan alopecia and its modification by corticosteroids. Arch Klin Exp Dermatol 1966, 226:13–20
10. Paus R: Therapeutic strategies for treating hair loss. Drug Discov Today Therap Strategies 2006, 3:101–110
11. Paus R, Handjiski B, Eichmuller S, Czarnetzki BM: Chemotherapy-induced alopecia in mice. Induction by cyclophosphamide, inhibition by cyclosporine A, and modulation by dexamethasone. Am J Pathol 1994, 144:719–734
12. Paus R, Schilli MB, Handjiski B, Menrad A, Henz BM, Plonka P: Topical calcitriol enhances normal hair regrowth but does not prevent chemotherapy-induced alopecia in mice. Cancer Res 1996, 56:4438–4443
13. Maurer M, Handjiski B, Paus R: Hair growth modulation by topical immunophilin ligands: induction of anagen, inhibition of massive catagen development, and relative protection from chemotherapy-induced alopecia. Am J Pathol 1997, 150:1433–1441
14. Ohnemus U, Unalan M, Handjiski B, Paus R: Topical estrogen accelerates hair regrowth in mice after chemotherapy-induced alopecia by favoring the dystrophic catagen response pathway to damage. J Invest Dermatol 2004, 122:7–13
15. Lindner G, Botchkarev VA, Botchkareva NV, Ling G, van der Veen C, Paus R: Analysis of apoptosis during hair follicle regression (catagen). Am J Pathol 1997, 151:1601–1617
16. Tobin DJ, Hagen E, Botchkarev VA, Paus R: Do hair bulb melanocytes undergo apoptosis during hair follicle regression (catagen)? J Invest Dermatol 1998, 111:941–947
17. Botchkarev VA, Komarova EA, Siebenhaar F, Botchkareva NV, Komarov PG, Maurer M, Gilchrest BA, Gudkov AV: p53 is essential for chemotherapy-induced hair loss. Cancer Res 2000, 60:5002–5006
18. Sharov AA, Li GZ, Palkina TN, Sharova TY, Gilchrest BA, Botchkarev VA: Fas and c-kit are involved in the control of hair follicle melanocyte apoptosis and migration in chemotherapy-induced hair loss. J Invest Dermatol 2003, 120:27–35
19. Botchkarev VA: Molecular mechanisms of chemotherapy-induced hair loss. J Investig Dermatol Symp Proc 2003, 8:72–75
20. Hussein AM, Jimenez JJ, McCall CA, Yunis AA: Protection from chemotherapy-induced alopecia in a rat model. Science 1990, 249:1564–1566
21. Jimenez JJ, Yunis AA: Protection from chemotherapy-induced alopecia by 1,25-dihydroxyvitamin D3. Cancer Res 1992, 52:5123–5125
22. Philpott MP, Green MR, Kealey T: Human hair growth in vitro. J Cell Sci 1990, 97:463–471
23. Hendrix S, Handjiski B, Peters EM, Paus R: A guide to assessing damage response pathways of the hair follicle: lessons from cyclophosphamide-induced alopecia in mice. J Invest Dermatol 2005, 125:42–51
24. Arnold H, Bourseaux F, Brock N: Chemotherapeutic action of a cyclic nitrogen mustard phosphamide ester (B 518-ASTA) in experimental tumours of the rat. Nature 1958, 181:931
25. Colvin OM: An overview of cyclophosphamide development and clinical applications. Curr Pharm Des 1999, 5:555–560
26. Connors TA, Cox PJ, Farmer PB, Foster AB, Jarman M: Some studies of the active intermediates formed in the microsomal metabolism of cyclophosphamide and isophosphamide. Biochem Pharmacol 1974, 23:115–129
27. Flowers J, Ludeman SM, Gamcsik MP, Colvin OM, Shao KL, Boal JH, Springer JB, Adams DJ: Evidence for a role of chloroethylaziridine in the cytotoxicity of cyclophosphamide. Cancer Chemother Pharmacol 2000, 45:335–344
28. Kehrer JP, Biswal SS: The molecular effects of acrolein. Toxicol Sci 2000, 57:6–15
29. Desmeules P, Devine PJ: Characterizing the ovotoxicity of cyclophosphamide metabolites on cultured mouse ovaries. Toxicol Sci 2006, 90:500–509
30. Orfanos CE, Gerstein E, Runne U: [Cytostatic hair loss as biological model. Cytostatic effect on healthy body cells.] German. Dtsch Med Wochenschr 1976, 101:1466–1468
31. Goldberg MT, Tackaberry LE, Hardy MH, Noseworthy JH: Nuclear aberrations in hair follicle cells of patients receiving cyclophosphamide. A possible in vivo assay for human exposure to genotoxic agents. Arch Toxicol 1990, 64:116–121
32. Slominski A, Tobin DJ, Shibahara S, Wortsman J: Melanin pigmentation in mammalian skin and its hormonal regulation. Physiol Rev 2004, 84:1155–1228
33. Slominski A, Wortsman J, Plonka PM, Schallreuter KU, Paus R, Tobin DJ: Hair follicle pigmentation. J Invest Dermatol 2005, 124:13–21
34. Slominski A, Paus R: Melanogenesis is coupled to murine anagen: toward new concepts for the role of melanocytes and the regulation of melanogenesis in hair growth. J Invest Dermatol 1993, 101:90S–97S
35. Slominski A, Paus R, Plonka P, Handjiski B, Maurer M, Chakraborty A, Mihm MC Jr: Pharmacological disruption of hair follicle pigmentation by cyclophosphamide as a model for studying the melanocyte response to and recovery from cytotoxic drug damage in situ. J Invest Dermatol 1996, 106:1203–1211
36. Tobin DJ, Slominski A, Botchkarev V, Paus R: The fate of hair follicle melanocytes during the hair growth cycle. J Investig Dermatol Symp Proc 1999, 4:323–332
37. Sharov AA, Siebenhaar F, Sharova TY, Botchkareva NV, Gilchrest BA, Botchkarev VA: Fas signaling is involved in the control of hair follicle response to chemotherapy. Cancer Res 2004, 64:6266–6270
38. Koch H, Wittern KP, Bergemann J: In human keratinocytes the common deletion reflects donor variabilities rather than chronologic aging and can be induced by ultraviolet A irradiation. J Invest Dermatol 2001, 117:892–897
39. Sung JS, Demple B: Roles of base excision repair subpathways in correcting oxidized abasic sites in DNA. FEBS J 2006, 273:1620–1629
40. Xu YJ, Kim EY, Demple B: Excision of C-4′-oxidized deoxyribose lesions from double-stranded DNA by human apurinic/apyrimidinic endonuclease (Ape1 protein) and DNA polymerase beta. J Biol Chem 1998, 273:28837–28844
41. Danilenko DM, Ring BD, Yanagihara D, Benson W, Wiemann B, Starnes CO, Pierce GF: Keratinocyte growth factor is an important endogenous mediator of hair follicle growth, development, and differentiation. Normalization of the nu/nu follicular differentiation defect and amelioration of chemotherapy-induced alopecia. Am J Pathol 1995, 147:145–154
42. Werner S: Keratinocyte growth factor: a unique player in epithelial repair processes. Cytokine Growth Factor Rev 1998, 9:153–165
43. Finch PW, Rubin JS: Keratinocyte growth factor/fibroblast growth factor 7, a homeostatic factor with therapeutic potential for epithelial protection and repair. Adv Cancer Res 2004, 91:69–136
44. Braun S, Krampert M, Bodo E, Born-Berclaz C, Paus R, Werner S: Keratinocyte growth factor protects epidermis and hair follicles from cell death induced by UV irradiation, chemotherapeutic or cytotoxic agents. J Cell Sci 2006, 119:4841–4849
45. Anderson LW, Ludeman SM, Colvin OM, Grochow LB, Strong JM: Quantitation of 4-hydroxycyclophosphamide/aldophosphamide in whole blood. J Chromatogr B Biomed Appl 1995, 667:247–257
46. Anderson LW, Chen TL, Colvin OM, Grochow LB, Collins JM, Kennedy MJ, Strong JM: Cyclophosphamide and 4-hydroxycyclophosphamide/aldophosphamide kinetics in patients receiving high-dose cyclophosphamide chemotherapy. Clin Cancer Res 1996, 2:1481–1487
47. Chen TL, Kennedy MJ, Anderson LW, Kiraly SB, Black KC, Colvin OM, Grochow LB: Nonlinear pharmacokinetics of cyclophosphamide and 4-hydroxycyclophosphamide/aldophosphamide in patients with metastatic breast cancer receiving high-dose chemotherapy followed by autologous bone marrow transplantation. Drug Metab Dispos 1997, 25:544–551
48. Magerl M, Paus R, Farjo N, Muller-Rover S, Peters EM, Foitzik K, Tobin DJ: Limitations of human occipital scalp hair follicle organ culture for studying the effects of minoxidil as a hair growth enhancer. Exp Dermatol 2004, 13:635–642
49. Bodó E, Bíró T, Telek A, Czifra G, Griger Z, Tóth BI, Mescalchin A, Ito T, Bettermann A, Kovács L, Paus R: A hot new twist to hair biology:

involvement of vanilloid receptor-1 (VR1/TRPV1) signaling in human hair growth control. Am J Pathol 2005, 166:985–998
50. Randall VA, Sundberg JP, Philpott MP: Animal and in vitro models for the study of hair follicles. J Investig Dermatol Symp Proc 2003, 8:39–45
51. Kwon OS, Oh JK, Kim MH, Park SH, Pyo HK, Kim KH, Cho KH, Eun HC: Human hair growth ex vivo is correlated with in vivo hair growth: selective categorization of hair follicles for more reliable hair follicle organ culture. Arch Dermatol Res 2006, 297:367–371
52. Stenn KS, Paus R: Controls of hair follicle cycling. Physiol Rev 2001, 81:449–494
53. Kligman AM: The human hair cycle. J Invest Dermatol 1959, 33: 307–316
54. Tobin DJ, Mandir N, Dover R: Morphological analysis of in vitro human hair growth. Arch Dermatol Res 1993, 285:158–164
55. Barbosa AJ, Castro LP, Margarida A, Nogueira MF: A simple and economical modification of the Masson-Fontana method for staining melanin granules and enterochromaffin cells. Stain Technol 1984, 59:193–196
56. Murata M, Suzuki T, Midorikawa K, Oikawa S, Kawanishi S: Oxidative DNA damage induced by a hydroperoxide derivative of cyclophosphamide. Free Radic Biol Med 2004, 37:793–802
57. Toyokuni S, Tanaka T, Hattori Y, Nishiyama Y, Yoshida A, Uchida K, Hiai H, Ochi H, Osawa T: Quantitative immunohistochemical determination of 8-hydroxy-2′-deoxyguanosine by a monoclonal antibody N45.1: its application to ferric nitrilotriacetate-induced renal carcinogenesis model. Lab Invest 1997, 76:365–374
58. Berneburg M, Kamenisch Y, Krutmann J, Rocken M: To repair or not to repair—no longer a question: repair of mitochondrial DNA shielding against age and cancer. Exp Dermatol 2006, 15:1005–1015
59. Lu Z, Hasse S, Bodo E, Rose C, Funk W, Paus R: Towards the development of a simplified long-term organ culture method for human scalp skin and its appendages under serum-free conditions. Exp Dermatol 2007, 16:37–44
60. Beattie PE, Finlan LE, Kernohan NM, Thomson G, Hupp TR, Ibbotson SH: The effect of ultraviolet (UV) A1, UVB and solar-simulated radiation on p53 activation and p21. Br J Dermatol 2005, 152:1001–1008
61. Berneburg M, Gremmel T, Kurten V, Schroeder P, Hertel I, von Mikecz A, Wild S, Chen M, Declercq L, Matsui M, Ruzicka T, Krutmann J: Creatine supplementation normalizes mutagenesis of mitochondrial DNA as well as functional consequences. J Invest Dermatol 2005, 125:213–220
62. Pfaffl MW: A new mathematical model for relative quantification in real-time RT-PCR. Nucleic Acids Res 2001, 29:e45
63. Müller-Röver S, Handjiski B, van der Veen C, Eichmuller S, Foitzik K, McKay IA, Stenn KS, Paus R: A comprehensive guide for the accurate classification of murine hair follicles in distinct hair cycle stages. J Invest Dermatol 2001, 117:3–15
64. Peters EM, Hansen MG, Overall RW, Nakamura M, Pertile P, Klapp BF, Arck PC, Paus R: Control of human hair growth by neurotrophins: brain-derived neurotrophic factor inhibits hair shaft elongation, induces catagen, and stimulates follicular transforming growth factor beta2 expression. J Invest Dermatol 2005, 124:675–685
65. Paus R, Foitzik K: In search of the "hair cycle clock": a guided tour. Differentiation 2004, 72:489–511
66. Tobin DJ, Foitzik K, Reinheckel T, Mecklenburg L, Botchkarev VA, Peters C, Paus R: The lysosomal protease cathepsin L is an important regulator of keratinocyte and melanocyte differentiation during hair follicle morphogenesis and cycling. Am J Pathol 2002, 160:1807–1821
67. Morioka K: Hair Follicle, Differentiation under the Electron Microscope. Tokyo, Springer, 2004
68. Vojtesek B, Bartek J, Midgley CA, Lane DP: An immunochemical analysis of the human nuclear phosphoprotein p53. New monoclonal antibodies and epitope mapping using recombinant p53. J Immunol Methods 1992, 151:237–244
69. Berneburg M, Grether-Beck S, Kurten V, Ruzicka T, Briviba K, Sies H, Krutmann J: Singlet oxygen mediates the UVA-induced generation of the photoaging-associated mitochondrial common deletion. J Biol Chem 1999, 274:15345–15349
70. Berneburg M, Plettenberg H, Medve-Konig K, Pfahlberg A, Gers-Barlag H, Gefeller O, Krutmann J: Induction of the photoaging-associated mitochondrial common deletion in vivo in normal human skin. J Invest Dermatol 2004, 122:1277–1283
71. Zaun H: Experimental studies on the pathogenesis of "mixed alopecia" in animals. Arch Klin Exp Dermatol 1964, 221:75–84
72. Dong Q, Barsky D, Colvin ME, Melius CF, Ludeman SM, Moravek JF, Colvin OM, Bigner DD, Modrich P, Friedman HS: A structural basis for a phosphoramide mustard-induced DNA interstrand cross-link at 5′-d(GAC). Proc Natl Acad Sci USA 1995, 92:12170–12174
73. Paus R, Cotsarelis G: The biology of hair follicles. N Engl J Med 1999, 341:491–497
74. Kern JC, Kehrer JP: Acrolein-induced cell death: a caspase-influenced decision between apoptosis and oncosis/necrosis. Chem Biol Interact 2002, 139:79–95
75. Liu-Snyder P, McNally H, Shi R, Borgens RB: Acrolein-mediated mechanisms of neuronal death. J Neurosci Res 2006, 84:209–218
76. Koppel RA, Boh EE: Cutaneous reactions to chemotherapeutic agents. Am J Med Sci 2001, 321:327–335
77. de Jonge ME, Mathot RA, Dalesio O, Huitema AD, Rodenhuis S, Beijnen JH: Relationship between irreversible alopecia and exposure to cyclophosphamide, thiotepa and carboplatin (CTC) in high-dose chemotherapy. Bone Marrow Transplant 2002, 30:593–597
78. Souid AK, Tacka KA, Galvan KA, Penefsky HS: Immediate effects of anticancer drugs on mitochondrial oxygen consumption. Biochem Pharmacol 2003, 66:977–987
79. Tacka KA, Dabrowiak JC, Goodisman J, Souid AK: Kinetic analysis of the reactions of 4-hydroperoxycyclophosphamide and acrolein with glutathione, mesna, and WR-1065. Drug Metab Dispos 2002, 30:875–882
80. Jia L, Liu Z, Sun L, Miller SS, Ames BN, Cotman CW, Liu J: Acrolein, a toxicant in cigarette smoke, causes oxidative damage and mitochondrial dysfunction in RPE cells: protection by (R)-α-lipoic acid. Invest Ophthalmol Vis Sci 2007, 48:339–348
81. Eicker J, Kurten V, Wild S, Riss G, Goralczyk R, Krutmann J, Berneburg M: Betacarotene supplementation protects from photoaging-associated mitochondrial DNA mutation. Photochem Photobiol Sci 2003, 2:655–659
82. Fischer TW, Sweatman TW, Semak I, Sayre RM, Wortsman J, Slominski A: Constitutive and UV-induced metabolism of melatonin in keratinocytes and cell-free systems. FASEB J 2006, 20:1564–1566
83. Lademann J, Otberg N, Jacobi U, Hoffman RM, Blume-Peytavi U: Follicular penetration and targeting. J Investig Dermatol Symp Proc 2005, 10:301–303
84. Hoffman RM: Topical liposome targeting of dyes, melanins, genes, and proteins selectively to hair follicles. J Drug Target 1998, 5:67–74
85. Li L, Hoffman RM: Topical liposome delivery of molecules to hair follicles in mice. J Dermatol Sci 1997, 14:101–108
86. Domashenko A, Gupta S, Cotsarelis G: Efficient delivery of transgenes to human hair follicle progenitor cells using topical lipoplex. Nat Biotechnol 2000, 18:420–423
87. Kawano M, Komi-Kuramochi A, Asada M, Suzuki M, Oki J, Jiang J, Imamura T: Comprehensive analysis of FGF and FGFR expression in skin: FGF18 is highly expressed in hair follicles and capable of inducing anagen from telogen stage hair follicles. J Invest Dermatol 2005, 124:877–885
88. Ohyama M, Terunuma A, Tock CL, Radonovich MF, Pise-Masison CA, Hopping SB, Brady JN, Udey MC, Vogel JC: Characterization and isolation of stem cell-enriched human hair follicle bulge cells. J Clin Invest 2006, 116:249–260
89. Kolehmainen J, Black GC, Saarinen A, Chandler K, Clayton-Smith J, Traskelin AL, Perveen R, Kivitie-Kallio S, Norio R, Warburg M, Fryns JP, de la Chapelle A, Lehesjoki AE: Cohen syndrome is caused by mutations in a novel gene, COH1, encoding a transmembrane protein with a presumed role in vesicle-mediated sorting and intracellular protein transport. Am J Hum Genet 2003, 72:1359–1369
90. Hashimoto T, Kazama T, Ito M, Urano K, Katakai Y, Yamaguchi N, Ueyama Y: Histologic and cell kinetic studies of hair loss and subsequent recovery process of human scalp hair follicles grafted onto severe combined immunodeficient mice. J Invest Dermatol 2000, 115:200–206
91. Botchkarev V, Sharov AA, Syska W, Maurer M, Gilchrest BA: Involvement of p53 and Fas in hair follicle apoptosis in human skin/SCID model for chemotherapy-induced hair loss. J Invest Dermatol 2002, 119:286
92. Ohnemus U, Uenalan M, Inzunza J, Gustafsson JA, Paus R: The hair follicle as an estrogen target and source. Endocr Rev 2006, 27:677–706